Determination of external surface composition of zeolite particles by synchrotron radiation XPS

Hiromichi Shimada, Nobuyuki Matsubayashi, Motoyasu Imamura, Toshio Sato and Akio Nishijima

National Institute of Materials and Chemical Research, 1-1 Higashi, Tsukuba, Ibaraki 305, Japan

Received 15 November 1995; accepted 14 February 1996

Non-destructive depth profiling analysis with high surface sensitivity was performed by XPS with synchrotron radiation excitation. Comparison of the measured atomic ratios with the simulated ones revealed the presence of a thin Al- and Na-rich overlayer at the external surface of NaY particles. For HY zeolite particles, a gradual decrease in the Al/Si ratio from the external surface to the bulk was observed.

Keywords: zeolite; XPS; depth profiling; synchrotron radiation

1. Introduction

The external surface properties of zeolite particles play important roles in many catalytic reactions, especially fluid catalytic cracking (FCC), because large molecules react predominantly on the external surface without entering the inner channels. In this context, a number of investigations [1–6] have been performed to reveal the external surface composition of zeolite particles using X-ray photoelectron spectroscopy (XPS) which has extensively been applied to the surface characterization of catalytic materials because of its capability to elucidate the chemical composition, chemical states and in-depth profile near the surface. However, in conventional XPS analyses employing characteristic X-ray sources such as Mg Kα (1253.6 eV) or Al Kα (1486.6 eV), the large inelastic mean free path (IMFP) of photoelectrons lowers the surface sensitivity, particularly in the analyses of photoelectrons with low binding energies (E_b). For instance, the IMFP values of Si 2p ($E_b \approx 100$ eV) and Al 2p ($E_b \approx 80$ eV) photoelectrons with Mg Kα excitation are calculated at longer than 30 Å in crystallized SiO_2 [7]. In the analysis of zeolites with polar structures, the average depth of analysis may reach almost 50 Å from the surface. The restriction of the surface sensitivity by large IMFP can be eliminated by the use of synchrotron radiation (SR) which is capable to provide energy-variable X-rays. In the present paper, we apply SR excited XPS to the determination of the external surface composition of zeolite particles. In addition to the surface sensitive XPS analysis, non-destructive depth profiling analysis is performed by changing the XPS excitation energy.

2. Experimental

All the XPS measurements were performed at the BL-13C of the Photon Factory at the National Laboratory for High Energy Physics. The beamline equipped with a spherical grating monochromator (SGM) [8,9] was coupled with a multi-purpose analytical chamber [10] at the most downstream. The entrance and exit slit width of the beamline was about 60 μm when the X-ray linewidth was about 0.4 eV at 200 eV and 1.0 eV at 800 eV. The XPS spectra were measured in the analytical chamber with a 180° hemispherical electrostatic analyzer (Rigaku XPS-7000), of which the axis was at an angle of 54.7° to the incident X-rays and normal to the sample surface. The analyzer was operated at a pass energy of 25 eV such that the total instrumental resolution did not cause the significant broadening of each spectrum. Under the above measurement conditions, it took less than 3 min to record each of Si 2p, Al 2p and Na 2s spectra with reasonable spectral resolution and high signal-to-noise ratios.

The zeolites analyzed in the present study were NaY and HY fine powders with a SiO_2/Al_2O_3 ratio of about 4.8, which were provided as reference catalysts by the Catalysis Society of Japan. The HY powders were prepared from the NaY powders through a triple ion-exchange followed by calcination at 400°C. Detailed description of these zeolites was already given elsewhere [6]. To minimize the charging, the zeolite powders were dispersed on stainless-steel sample holding plates using a sonicator.

3. Results and discussion

Fig. 1 shows the Si 2p, Al 2p and Na 2s XPS spectra

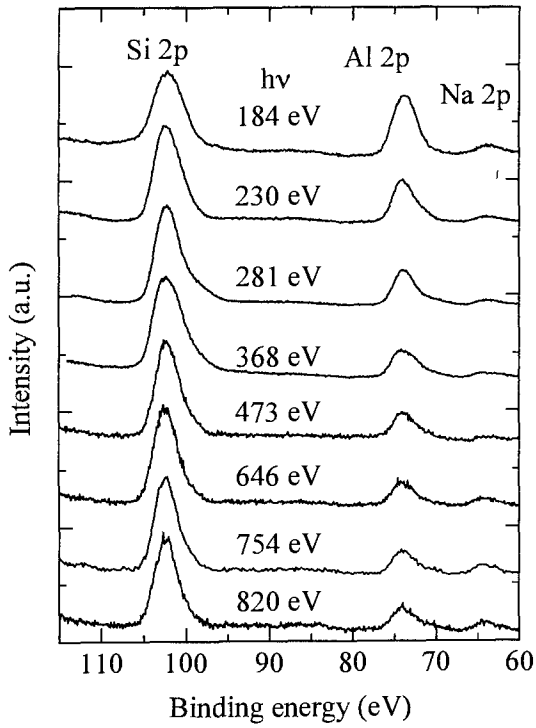

Fig. 1. Si 2p, Al 2p and Na 2s XPS spectra of NaY measured with different excitation energies.

of NaY measured at different excitation energies between 184 and 820 eV. In the above excitation energy range, the photoionization cross sections for the Na, Al and Si 2p subshells are significantly larger than those for the 2s subshells [11]. Accordingly, it is advantageous to measure the 2p spectra for the calculation of the Al/Si and Na/Al atomic concentration ratios. Nevertheless, for the determination of the Na concentration, the intensity of the 2s spectrum has been used instead of the 2p spectrum, because the Na 2p spectrum is interfered by the O 2s spectrum. The energy shift caused by charging has been corrected in fig. 1 such that the Si 2p spectrum has a peak at 102.5 eV. In addition, the spectral intensities are normalized at the peak intensity of Si 2p.

Fig. 1 demonstrates the changes of relative peak intensities of Al 2p and Na 2s relative to Si 2p with excitation energy. To quantitatively analyze the Al/Si and Na/Si atomic ratios, the Al 2p/Si 2p and Na 2s/Al 2p peak intensity ratios are calculated and plotted as a function of excitation energy in fig. 2. Each peak intensity has been obtained by integrating the peak area after subtracting the background using the Shirley method [12]. Fig. 2 clearly displays that both Al 2p/ Si 2p and Na 2s/ Si 2p ratios decrease with increasing excitation energy up to 473 eV. Further increase in excitation energy gives rise to the intensity of Na 2s, while the intensity of Al 2p remains almost constant at excitation energies over 473 eV.

For further discussion, it is necessary to convert the scales on the ordinate and abscissa to the atomic ratio

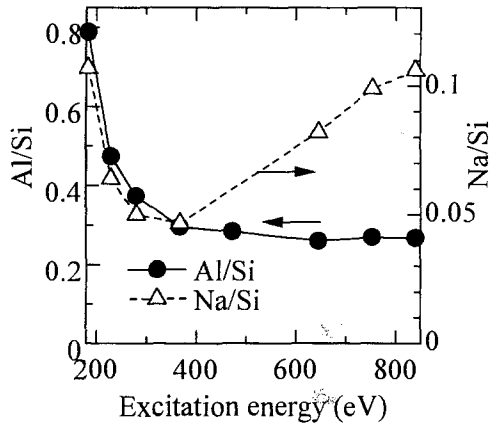

Fig. 2. Change in Al 2p/Si 2p and Na 2s/Si 2p XPS peak intensity ratios of NaY with excitation energy.

and IMFP, respectively. The atomic ratio can be obtained by the following equation:

$$n\left(\frac{\mathrm{X}}{\mathrm{Si}}\right)_{h\nu} = \frac{S_{\mathrm{X}}(h\nu)/\sigma_{\mathrm{X}}(h\nu)}{S_{\mathrm{Si}}(h\nu)/\sigma_{\mathrm{Si}}(h\nu)}, \quad (1)$$

where X is Al or Na and $n(\mathrm{X/Si})_{h\nu}$ is the atomic ratio of X relative to Si obtained at an excitation energy of $h\nu$. $S_{\mathrm{X}}(h\nu)$ ($S_{\mathrm{Si}}(h\nu)$) and $\sigma_{\mathrm{X}}(h\nu)$ ($\sigma_{\mathrm{Si}}(h\nu)$) denote, respectively, the peak intensity and the calculated photoionization cross section [11] for the spectrum of X (Si) at an excitation energy of $h\nu$. The IMFP values of the photoelectrons at each excitation energy have been calculated using the modified Bethe equation for SiO_2 [7] with the theoretical density of Y zeolite of 1.27 g/cm^3 instead of 2.19 g/cm^3 of pure SiO_2. Since the binding energies of Si 2p and Na 2s are close to that of Al 2p, the IMFP values for Si 2p and Na 2s photoelectrons are assumed to be the same as that for Al 2p.

Fig. 3 shows thus calculated Al/Si and Na/Si atomic ratios of NaY plotted as a function of IMFP. In fig. 3, steep increases in the Al/Si and Na/Si ratios are observed with decreasing IMFP below 20 Å. This suggests the presence of an Al- and Na-rich overlayer at the

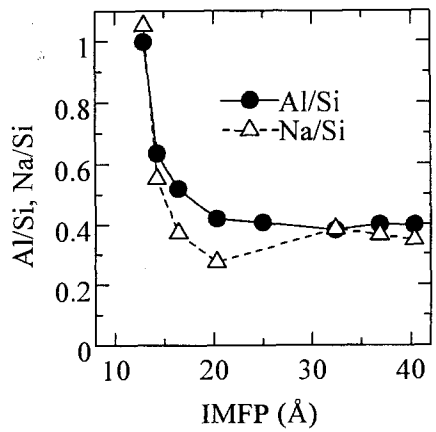

Fig. 3. Plots of Al/Si and Na/Si atomic ratios of NaY as a function of IMFP.

external surface of the NaY particles. Fig. 3 also indicates that the Al/Si and Na/Si ratios are almost equivalent, independent of the IMFP. This is consistent with the characteristics of NaY zeolite, in which Na is located adjacent to Al to compensate the negative charge. Small discrepancy between the Al/Si and Na/Si ratios is presumably due to the relative error in the calculated photoionization cross sections of Na 2s relative to Al 2p.

As a next step of analysis, the Al/Si ratio profile has been simulated using a model that is shown in the insertion of fig. 4. In this model, an Al-rich overlayer with a thickness of t Å and an Al/(Si + Al) atomic ratio of a_0 covers homogeneously NaY particles with an Al/(Si + Al) atomic ratio of a_1. The following assumptions are made in the simulation [13]: (i) attenuation length of the photoelectrons is identified by IMFP; (ii) attenuation of photoelectron flux is exponential in the normal direction to the sample surface. On these assumptions, the Al/Si atomic ratio obtained at an IMFP value of l Å, $n(\mathrm{Al/Si})_l$, is given by the following equation:

$$n\left(\frac{\mathrm{Al}}{\mathrm{Si}}\right)_l = \frac{\int_0^t a_0 e^{-z/l}\,dz + \int_t^\infty a_1 e^{-z/l}\,dz}{\int_0^t (1-a_0)e^{-z/l}\,dz + \int_t^\infty (1-a_1)e^{-z/l}\,dz} = \frac{a_0 - (a_0 - a_1)e^{-t/l}}{(1-a_0) + (a_0 - a_1)e^{-z/l}}. \quad (2)$$

Fig. 4 displays the comparison of the experimentally obtained n(Al/Si) ratios with the simulated profiles by the above equation. The n(Al/Si) ratios recorded with Al Kα and Mg Kα excitation are also plotted as experimentally obtained data. The n(Al/Si) ratios of 0.36–0.37 obtained with Al Kα and Mg Kα excitation are in good agreement with the value of 0.38 reported in a previous report [6].

The almost constant n(Al/Si) ratio over 30 Å of IMFP in the experimental data determines the bulk Al/(Si + Al) atomic ratio, a_1, almost unambiguously to be about 0.25, which is a little smaller than that obtained by chemical analysis of the same NaY zeolite of 0.30 [6]. The discrepancy is within a calculation error in quantitative XPS analyses. In fig. 4, two simulated profiles are given with the parameter sets of $a_0 = 1.0$, $a_1 = 0.25$, $t = 2$ and $a_0 = 0.8$, $a_1 = 0.25$, $t = 2$. As evidently observed, good fit is not attained in the low IMFP region in either case. The discrepancy is predominantly due to the overestimation of IMFP for the experimentally obtained data in the small IMFP region.

Recent studies have revealed that the above assumptions (i) and (ii) may not be correct for low-energy electrons because electron elastic scattering significantly affects electron trajectories in solids [14,15]. As a result, the contribution from the overlayer in total XPS signals is larger than that estimated simply using the IMFP values in the literature [7]. In other words, average depth of analysis in the small IMFP region is overestimated in the above assumptions (i) and (ii). The correction of the IMFP for the experimentally obtained data would significantly reduce the discrepancy between the measured and simulated profiles in fig. 4, although it is impossible to use a better equation instead of eq. (2) at this moment. Nevertheless, the simulation results clearly indicate that a very thin overlayer which scarcely contains Si covers the external surface of the NaY particles.

Fig. 5 displays the Al/Si atomic ratios of HY plotted as a function of IMFP that have been calculated by the same procedure as described above. In contrast to NaY, the Al/Si ratio of HY decreases gradually with increasing IMFP. This profile suggests a continuous decrease in the Al/Si ratio with the depth from the surface. In this context, the Al/Si ratios have been simulated using a model displayed in the insertion of fig. 5. In this model,

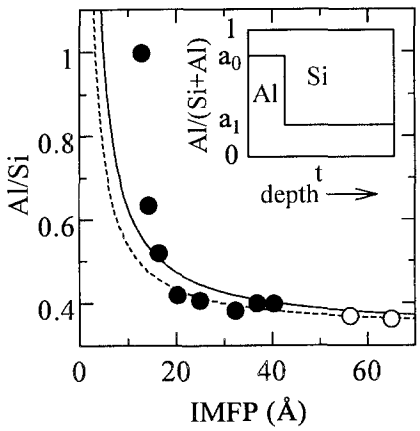

Fig. 4. Comparison between measured and simulated Al/Si ratios of NaY as a function of IMFP. The solid circles represent the measured ratios with SR excitation and the open circles the measured ratios with Mg Kα and Al Kα excitation. The solid line denotes the simulated ratios with $a_0 = 1$, $a_1 = 0.25$ and $t = 2$ and the dashed line the simulated ratios with $a_0 = 0.8$, $a_1 = 0.25$ and $t = 2$.

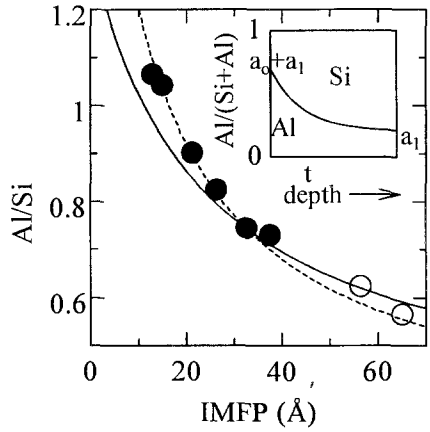

Fig. 5. Comparison between measured and simulated Al/Si ratios of HY as a function of IMFP. The solid circles represent the measured ratios with SR excitation and the open circles the measured ratios with Mg Kα and Al Kα excitation. The solid line denotes the simulated ratios with $a_0 = 0.32$, $a_1 = 0.25$ and $t = 40$ and the dashed line the simulated result with $a_0 = 0.43$, $a_1 = 0.23$ and $t = 27$.

the Al/(Si + Al) atomic ratio at the depth of z Å from the surface, $I_{Al}(z)$, is described by the following equation:

$$I_{Al}(z) = a_0\, e^{-z/t} + a_1\,, \tag{3}$$

where the Al/(Si + Al) ratio at the external surface is given as $a_0 + a_1$ and that in the bulk given as a_1, assuming that t Å is much smaller than the particle size. Upon the same assumptions as used for the calculation of eq. (2), the $n(\mathrm{Al/Si})_l$ is given by the following equation:

$$n\left(\frac{\mathrm{Al}}{\mathrm{Si}}\right)_l = \frac{\int_0^\infty (a_0 e^{-z/t} + a_1) e^{-z/l}\, dz}{\int_0^\infty (1 - a_0 e^{-z/t} - a_1) e^{-z/l} dz} = \frac{a_1 + a_0 t/(t+l)}{(1-a_1) - a_0 t/(t+l)}\,. \tag{4}$$

In previous literature [6], the bulk Al/(Si + Al) ratio of the HY powders was reported to be 0.28 by chemical analysis, which was a little smaller than that of NaY. Thus, the a_1 value in the simulation has been assumed to be from 0.23 to 0.25. Two simulated profiles are shown in fig. 5 with parameter sets of $a_0 = 0.32$, $a_1 = 0.25$, $t = 40$ and $a_0 = 0.43$, $a_1 = 0.23$, $t = 27$. Considerably good fits are obtained in both cases, though the IMFP values of the experimentally obtained data in the small IMFP region are also overestimated, as discussed above. The simulation results indicate that the Al/(Si + Al) ratio at the external surface of the HY particles reaches about 0.6 and decreases gradually with increasing the depth from the surface.

In summary, the SR-XPS analysis has revealed the presence of a very thin (~ 5 Å) overlayer with an extremely low silicon content, likely $NaAlO_2$, around the NaY particles. During the ion-exchange and following procedures, the overlayer of NaY is removed. Instead, enrichment of Al has occurred at the external part of the HY particles. A question remains if the high Al/Si ratio at the external surface of HY is resulted from the presence of amorphous alumina or high Al/Si zeolite. Finally, it should be noted that the present method is particularly useful for the characterization of catalysts of which external surface plays an important role in catalysis.

Acknowledgement

This work has been performed under the approval of the Photon Factory Advisory Committee (No. 94G-184).

References

[1] J.-Fr. Tempere, D. Delafosse and J.P. Contour, Chem. Phys. Lett. 33 (1975) 95.
[2] J. Finster and P. Lorenz, Chem. Phys. Lett. 50 (1977) 223.
[3] S.J. Kulkarni, S. Badrinarayan and S.B. Kulkarni, J. Catal. 75 (1982) 423.
[4] Th. Gross, U. Lohse, G. Engelhardt, K.-H. Richter and V. Patzelova, Zeolites 4 (1984) 25.
[5] V. Andera, L. Kubelkova, J. Novakova, B. Wichterlova and S. Bednarova, Zeolites 5 (1985) 67.
[6] Y. Okamoto, M. Ogawa, A. Maezawa and T. Imanaka, J. Catal. 112 (1988) 427.
[7] S. Tanuma, C.J. Powell and D.R. Penn, Surf. Interf. Anal. 17 (1991) 927.
[8] N. Matsubayashi, H. Shimada, K. Tanaka, T. Sato, Y. Yoshimura and A. Nishijima, Rev. Sci. Instr. 63 (1992) 1363.
[9] H. Shimada, N. Matsubayashi, Y. Imamura, K. Tanaka, T. Sato, Y. Yoshimura, T. Hayakawa, K. Talehira, A. Toyoshima, K. Tanaka and A. Nishijima, Rev. Sci. Instr. 66 (1995) 1780.
[10] N. Matsubayashi, I. Kojima, M. Kurahashi, A. Nishijima, A. Itoh and T. Utaka, Rev. Sci. Instr. 60 (1989) 2533.
[11] J.J. Yeh and I. Lindau, At. Data Nucl. Data Tables 32 (1985) 155.
[12] D.A. Shirley, Phys. Rev. B 5 (1972) 4709.
[13] H. Shimada, N. Matsubayashi, Y. Imamura, T. Sato and A. Nishijima, Appl. Surf. Sci., in print.
[14] A. Jablonski, Surf. Interf. Anal. 20 (1993) 771.
[15] A. Jablonski and S. Tougaard, J. Vac. Sci. Technol. 8 (1990) 106.